The Rule-based Conceptual Design of the Architecture of Serial Schönflies-motion Generators

Stéphane Caro⋆

stephane.caro@irccyn.ec-nantes.fr

Waseem Ahmad Khan† **Damiano Pasini**‡ **Jorge Angeles**‡

waseem@robotmaster.com damiano.pasini@mcgill.ca angeles@cim.mcgill.ca

⋆ Institut de Recherche en Communications et Cybernétique de Nantes

UMR CNRS n° 6597

1 rue de la Noë, 44321 Nantes, France

† Jabez Technologies Inc.

5929 Rte Transcanadienne, suite 320, St. Laurent, QC, H4T 1Z6 Canada

‡ Department of Mechanical Engineering & Centre for Intelligent Machines

McGill University

817 Sherbrooke West, Montreal, QC, H3A 2K6 Canada

Abstract

The conceptual design of manipulator architectures, the subject of this paper, pertains to the *topology* of the underlying kinematic chain. Schönflies Motion Generators (SMGs) are manipulators which are capable of a special class of motions—three independent translations and one rotation about an axis of fixed direction. In this paper, *synthesis rules* are proposed to obtain a complete minimum set of serial topologies capable of producing Schönflies motion. Only *revolute* R, *prismatic* P, *helical* H and Π joints are considered, as any multi-degree-of-freedom lower kinematic pair can be produced as a combination of R, P and H joints. Next, the *concept-evaluation framework*, proposed in an earlier work, is used to organize the topologies obtained in an ascending order of *complexity*, hence completing the conceptual design phase of the subject motion generators.

1 Introduction

The conceptual design of the architecture of a mechanical system aims at defining the topology of the associated kinematic chain. Schönflies-Motion Generators (SMGs) are manipulators which are capable of a special class of motions, those produced with serial robots termed SCARA (Selective-Compliance Assembly Robot Arm): three independent translations and one rotation about an axis of fixed direction, similar to the motions undergone by the tray of a waiter. Such motions, termed *Schönflies*, are known to stem from a displacement *subgroup* of rigid-body motions, termed the *Schönflies subgroup* [1, 2, 3]. The set of displacements of Schönflies motions is endowed with the algebraic properties of a *group* [4].

SMGs produce four-degree-of-freedom (four-dof) displacements of their end-effector (EE). This set of displacements was first studied by the German mathematician-mineralogist Arthur Moritz Schönflies (1853–1928). For this reason, the set of such motions is known to geometers as the Schönflies subgroup of the group of rigid-body displacements [5].

A list of serial SMGs was produced by Lee and Hervé [3, 6] based on the Lie-group-algebraic properties of the displacement set. However, Lee and Hervé's list does not contain manipulators with Π-joints. The latter are also called *parallelogram* joints because a Π-joint is a four-bar linkage with its opposite links of the same lengths. Although it might appear counterintuitive to regard the parallelogram linkages of interest as joints, the term is completely justified, as these joints (i) have appeared in many industrial robots, notably those with the Delta architecture [7] and the Quattro [8]; (ii) are well documented in the technical literature [9, 10, 11]; and (iii) have been studied systematically as valuable means in parallel-robot design [4].

In this paper, *synthesis rules* are proposed to obtain a complete minimum set of serial topologies capable of producing Schönflies motion. Only *revolute* R, *prismatic* P, *helical* H and Π joints are considered. In fact, any of the remaining lower kinematic pairs (LKPs) can be synthesized as a combination of R, P and H joints. Next, the *concept-evaluation framework*, proposed in an earlier work, is used to organize the topologies obtained in an ascending order of *complexity*, hence completing the conceptual design phase of the subject motion generators.

2 Kinematic Bond, Kinematic Chain and Kinematic Pair

It is known [2] that the set of rigid-body displacements $\mathcal{D}$ has the algebraic structure of a group. Moreover, $\mathcal{D}$ includes interesting and practical subgroups that find relevant applications in the design of production-automation and prosthetic devices. The combination of subgroups, in general, can take place via the standard set operations of union and intersection. The set defined as that comprising the elements of two displacement subgroups is not necessarily a subgroup, and hence, one cannot speak of the union of displacement subgroups. On the contrary, the intersection of two displacement subgroups is always a subgroup itself, and hence, the intersection of displacement subgroups is a valid group operation. Rather than the union of groups, what we have is the product of groups [12]. Let $\mathcal{G}_1$ and $\mathcal{G}_2$ be two groups defined over the same binary operation $\star$; if $g_1 \in \mathcal{G}_1$ and $g_2 \in \mathcal{G}_2$, then the product of these two groups, represented by $\mathcal{G}_1 \bullet \mathcal{G}_2$, is the set of elements of the form $g_1 \star g_2$. Here, the order is important, as commutativity is not to be taken for granted in group theory, i.e., in general, $\mathcal{G}_1 \bullet \mathcal{G}_2 \neq \mathcal{G}_2 \bullet \mathcal{G}_1$.

The intersection of the two foregoing groups, represented by the usual set-theoretic symbol $\cap$, i.e., $\mathcal{G}_1 \cap \mathcal{G}_2$, is the group of elements g belonging to both $\mathcal{G}_1$ and $\mathcal{G}_2$, and hence, the order is not important. Thus, $\mathcal{G}_1 \cap \mathcal{G}_2 = \mathcal{G}_2 \cap \mathcal{G}_1$.

A total of 12 displacement subgroups of the group of rigid-body displacements was first listed by Hervé [13]. For quick reference, we reproduce Hervé's list below:

1. $\mathcal{R}(\mathcal{A})$, the subgroup of rotations about axis [1] $\mathcal{A}$;

2. $\mathcal{P}(\mathbf{e})$, the subgroup of translations along the direction $\mathbf{e}$;

3. $\mathcal{H}(\mathcal{A}, p)$, the subgroup of rotations through an angle ϕ about axis $\mathcal{A}$ and translations u along the direction of the same axis, translations and rotations being related by the pitch p in the form $u = p\phi$;

4. $\mathcal{C}(\mathcal{A})$, the subgroup of independent rotations about and translations in the direction of axis $\mathcal{A}$;

5. $\mathcal{F}(\mathbf{u}, \mathbf{v})$, the subgroup of two independent translations in the directions of the distinct unit vectors $\mathbf{u}$ and $\mathbf{v}$, and one rotation about an axis normal to both $\mathbf{u}$ and $\mathbf{v}$;

6. $\mathcal{S}(O)$, the subgroup of rotations about point O.

7. $\mathcal{I}$, the identity subgroup;

8. $\mathcal{T}_2(\mathbf{u}, \mathbf{v})$, the planar-translation subgroup of translations in the directions of the two distinct unit vectors $\mathbf{u}$ and $\mathbf{v}$;

9. $\mathcal{T}_3$, the translation subgroup of translations in 3D space;

10. $\mathcal{Y}(\mathbf{e}, p)$, the subgroup of motions allowed by a screw of pitch p and axis parallel to $\mathbf{e}$ undergoing arbitrary translations in a direction normal to $\mathbf{e}$;

[1] An axis being a line, $\mathcal{A}$ is fully determined by either a point and a direction or two points.

11. $\mathcal{X}(\mathbf{u}) = \mathcal{F}(\mathbf{v}, \mathbf{w}) \bullet \mathcal{P}(\mathbf{u})$, the subgroup resulting of the product of the planar subgroup of plane normal to $\mathbf{u}$, i.e., $\mathbf{v} \cdot \mathbf{u} = \mathbf{w} \cdot \mathbf{u} = 0$, and the prismatic subgroup of direction $\mathbf{u}$. Each element of this subgroup is thus characterized by the two translations t_v, t_w and the angle ϕ of the planar subgroup plus the translation t_u in the direction of $\mathbf{u}$. This subgroup is known as the Schönflies subgroup;

12. $\mathcal{D}$, the set of rigid-body displacements, each of whose elements is characterized by three independent translations and three independent rotations.

A *kinematic bond* is defined as a set of displacements stemming from the product of displacement subgroups, [4, 13]. Notice that a bond itself need not be a subgroup. For example, the *universal bond*

$$\mathcal{U}(O) = \mathcal{R}(\mathcal{A}_1) \bullet \mathcal{R}(\mathcal{A}_2) \tag{1}$$

where $\mathcal{A}_1$ and $\mathcal{A}_2$ are two axes intersecting at point O at right angles, is not a subgroup. The name of this bond derives from its mechanical realization, namely, the universal joint. We denote a kinematic bond by $\mathcal{L}(i, n)$, where i and n stand for the integer numbers associated with the two end links of the bond.

A kinematic bond is realized by a *kinematic chain*, which is the result of the coupling of rigid bodies, called links, via *kinematic pairs*. When the coupling takes place in such a way that the two links share a common surface, a *lower kinematic pair* results; when the coupling takes place along a common line or a common point, a *higher kinematic pair* arises. Examples of higher kinematic pairs include gears and cams. Π-joints are a special kind, not belonging to either lower- nor higher-kinematic pairs. We shall denote the subgroup associated with the lower kinematic pair coupling links i and $i+1$ as $\mathcal{L}(i, i+1)$, a kinematic bond $\mathcal{L}(i, n)$ being obtained from the product of $n - i$ such subgroups, i.e.,

$$\mathcal{L}(i, n) = \mathcal{L}(i, i+1) \bullet \mathcal{L}(i+1, i+2) \bullet \cdots \bullet \mathcal{L}(n-1, n) \tag{2}$$

There are six basic lower kinematic pairs, namely (1) revolute R, (2) prismatic P, (3) helical H, (4) cylindrical C, (5) planar F, and (6) spherical S. These pairs are the generators of the displacement subgroups $\mathcal{R}(\mathcal{A})$, $\mathcal{P}(\mathbf{e})$, $\mathcal{H}(\mathcal{A}, p)$, $\mathcal{C}(\mathcal{A})$, $\mathcal{F}(\mathbf{u}, \mathbf{v})$ and $\mathcal{S}(O)$, respectively. Although the foregoing displacement subgroups can be realized by their corresponding lower kinematic pairs, it is often possible to realize the displacement subgroups by appropriate kinematic chains. A common example is that of $\mathcal{C}(\mathcal{A})$ which, besides the C pair, can be realized by a suitable concatenation of a P and a R pair [14].

In addition to the first three lower kinematic pairs, we consider the Π-joint [9, 10, 15], a parallelogram four-bar linkage, when synthesizing a SMG.

3 Type Synthesis of a Serial SMG

In this section we introduce a novel method to identify the motions generated by a kinematic bond based on the displacement subgroups. This method is then used to produce a list of Schönflies-Motion Generators. As we focus on serial SMGs, let us introduce three premises:

Premise 1 *Only manipulators composed of a combination of* R*,* P*,* H *and* Π *joints are considered.*

Premise 2 *All* R *and* H *joints composing a serial SMG must have their axes parallel.*

Premise 3 *The direction of a* P *joint*[2] *need not be normal to the other joint axes composing a serial SMG.*

The combination of subgroups, in general, can take place via the group product operation. Now we introduce

Definition 1 *A kinematic chain composed of kinematic pairs* R*,* P*,* H *of axes parallel to vector* $\mathbf{u}$ *is said to be a* class-$\mathcal{X}_\mathbf{u}$ chain*.*

For brevity, in the balance of the paper we denote by $\mathsf{R}_\mathbf{u}$ any revolute pair of axis parallel to a unit vector $\mathbf{u}$, the same notation applying to $\mathsf{H}_\mathbf{u}$. Furthermore, two $\mathsf{H}_\mathbf{u}$ pairs of a class-$\mathcal{X}_\mathbf{u}$ chain are assumed to have distinct pitches, unless otherwise stated. $\mathsf{P}_\mathbf{u}$ denotes, in turn, a prismatic pair with direction parallel to the unit vector $\mathbf{u}$.

Definition 2 *The* dimension *of a group is the number of independent variables that uniquely describe one member of the group. When a kinematic bond is a group, its dimension is the degree of freedom of the underlying kinematic chain.*

Moreover, the concept of dimension is readily extended to a kinematic bond, namely,

Definition 3 *The* dimension *of a kinematic bond is the number of independent variables that uniquely describe one member of the bond. The dimension of a kinematic bond is the degree of freedom of the kinematic chain that realizes the bond.*

For example, for the bond $\mathcal{U}$ introduced in eq.(1),

$$\dim(\mathcal{U}) = 2$$

[2] P joints do not have an axis, but only a *direction*. For a terser discussion, we refer sometimes to the "axis" of a P joint, the implication being that a *direction* is meant.

Assuming two kinematic bonds $\mathcal{L}_1$ and $\mathcal{L}_2$, it is noteworthy that:

$$\dim\{\mathcal{L}_1 \bullet \mathcal{L}_2\} \leq \dim\{\mathcal{L}_1\} + \dim\{\mathcal{L}_2\} \tag{3}$$

$$\dim\{\mathcal{L}_1 \cap \mathcal{L}_2\} \leq \min\{\dim\{\mathcal{L}_1\}, \dim\{\mathcal{L}_2\}\} \tag{4}$$

As an illustration of inequality (3), let us define $\mathcal{L}_i$ as $\mathcal{S}(O_i)$, for $i = 1, 2$, O_i denoting one point O_i. One has

$$\dim[\mathcal{S}(O_i)] = 3, \quad i = 1, 2;$$

and

$$\dim[\mathcal{S}(O_1) \bullet \mathcal{S}(O_2)] = 5 < \dim[\mathcal{S}(O_1)] + \dim[\mathcal{S}(O_2)] = 6$$

That is, the dof of a serial array of two spherical joints is five, as the kinematic bond thus resulting—not a subgroup—is short of one dof to allow its end link a full six-dof motion: the end link is prevented from translating in the direction of the segment $\overline{O_1 O_2}$.

To illustrate inequality (4), let us define $\mathcal{L}_1$ as $\mathcal{R}(\mathcal{A}_1)$ and $\mathcal{L}_2$ as $\mathcal{C}(\mathcal{A}_2)$, with $\mathcal{A}_1$ and $\mathcal{A}_2$ defined, in turn, as two *parallel* lines. Thus,

$$\dim[\mathcal{R}(\mathcal{A}_1)] = 1, \quad \dim[\mathcal{C}(\mathcal{A}_2)] = 2, \quad \dim[\mathcal{R}(\mathcal{A}_1) \cap \mathcal{C}(\mathcal{A}_2)] = 0$$

Indeed, the parallel array of one R and one C joints, of parallel axes constrains completely the two coupled links, the kinematic chain of interest then degenerating into one isostatic structure.

Accordingly,

Lemma 1 *The degree of freedom of a Parallel Kinematics Machine (PKM) with l limbs is, at most, equal to the dof of its limb with the lowest mobility.*

4 Rules for the Type-Synthesis of Serial SMGs

This section aims at defining a set of rules for the type-synthesis of serial SMGs composed of only R, P, H and Π-joints. Let $\mathcal{X}(\mathbf{u})$ be the required Schönflies motion, i.e., the Schönflies subgroup about an axis parallel to the unit vector $\mathbf{u}$. In this vein, we provide below a set of rules in the form of lemmas and corollaries.

Lemma 2 *The bond produced by any lower kinematic pair is idempotent, i.e., if $\mathcal{L}(\cdot)$ represents any of these bonds, then*

$$\mathcal{L}(\cdot) \bullet \mathcal{L}(\cdot) = \mathcal{L}(\cdot)$$

Consequently,

Corollary 1 *All twelve subgroups of $\mathcal{D}$ are idempotent.*

In particular, as far as Schönflies motion generation is concerned,

$$\mathcal{R}(\mathcal{A}) \bullet \mathcal{R}(\mathcal{A}) = \mathcal{R}(\mathcal{A})$$

$$\mathcal{P}(\mathbf{u}) \bullet \mathcal{P}(\mathbf{u}) = \mathcal{P}(\mathbf{u})$$

$$\mathcal{H}(\mathcal{A}, p) \bullet \mathcal{H}(\mathcal{A}, p) = \mathcal{H}(\mathcal{A}, p)$$

$\mathcal{A}$ being the axis of the corresponding pair, $\mathbf{u}$ its direction and p the pitch of the H pair.

However, the product of two identical $\mathit{\Pi}$-bonds[3] (serial array) is $\mathcal{T}_2$, i.e.,

$$\mathit{\Pi}_{\mathbf{n}} \bullet \mathit{\Pi}_{\mathbf{n}} = \mathcal{T}_2(\mathbf{n})$$

$\mathbf{n}$ being the axis normal to the plane of the two Π joints generating the two identical $\mathit{\Pi}_{\mathbf{n}}$ bonds. From Corollary 1, it is apparent that:

Corollary 2 *If a kinematic bond is a subgroup, then it is idempotent.*

A kinematic bond that is not a subgroup is not necessarily idempotent.

Lemma 3 *If a kinematic bond contains two prismatic pairs, of non-parallel directions, introducing a third prismatic pair of direction contained in the plane spanned by the direction vectors of the first two pairs does not affect the mobility of the original bond, e.g.*

$$\mathcal{P}(\mathbf{u}) \bullet \mathcal{P}(\mathbf{v}) \bullet \mathcal{P}(\mathbf{x}) = \mathcal{P}(\mathbf{u}) \bullet \mathcal{P}(\mathbf{v}) = \mathcal{T}_2(\mathbf{u}, \mathbf{v}), \quad \mathbf{x} \cdot (\mathbf{u} \times \mathbf{v}) = 0$$

Lemma 4 *The product of the bonds (subgroups, in this case) generated by coaxial revolute and cylindrical joints results in the same cylindrical bond:*

$$\mathcal{R}(\mathcal{A}) \bullet \mathcal{C}(\mathcal{A}) = \mathcal{C}(\mathcal{A})$$

Lemma 5 *All revolute, cylindrical and helical joints of a serial chain must have their axes parallel in order to produce the Schönflies motion group $\mathcal{X}(\mathbf{u})$.*

While, in general, the group product is not commutative,

Lemma 6 *The product of any pair of bonds generated by a class-$\mathcal{X}_{\mathbf{u}}$ chain is commutative.*

[3] The bond of the Π-joint is denoted by a subscripted italic $\mathit{\Pi}$, the subscript denoting the unit vector normal to the plane of the joint.

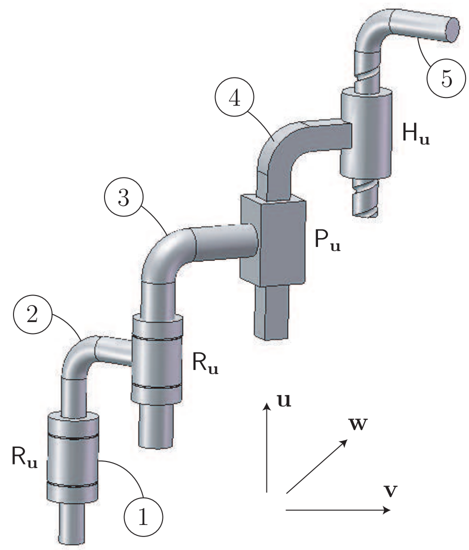

Figure 1: $\mathsf{R}_\mathbf{u}\,\mathsf{R}_\mathbf{u}\,\mathsf{P}_\mathbf{u}\,\mathsf{H}_\mathbf{u}$ manipulator

As a consequence of Lemma 6,

Corollary 3 *The product of n kinematic bonds generated by n class-$\mathcal{X}_\mathbf{u}$ chains is immutable under a bond permutation.*

Corrolary 3 implies that all chains obtained by a reordering of the joints generating $\mathcal{X}(\mathbf{u})$ are equivalent in terms of bond-generation. For example, let us assume five links, numbered from 1 to 5, and coupled by four kinematic pairs, as shown in Fig. 1, all of the $\mathcal{X}_\mathbf{u}$-class. Due to the commutativity of the product operation within a displacement subgroup, then, any permutation of the joints of the kinematic chain of Fig. 1 is a SMG, generating the same $\mathcal{X}(\mathbf{u})$ subgroup. Now we have

Lemma 7 *The minimum number of joints of the $\mathcal{X}_\mathbf{u}$-class or of the $\Pi_\mathbf{n}$ type, with $\mathbf{n}$ normal to $\mathbf{u}$, composing a SMG is four.*

Let us introduce one more definition:

Definition 4 *Given two mutually orthogonal unit vectors $\mathbf{u}$ and $\mathbf{n}$, the set $\mathcal{S}_\mathbf{u}$ is defined as*

$$\mathcal{S}_\mathbf{u} = \{\, \mathsf{R}_\mathbf{u}, \mathsf{P}_\mathbf{u}, \mathsf{H}_\mathbf{u}, \Pi_\mathbf{n} \,\} \tag{5}$$

That is, $\mathcal{S}_\mathbf{u}$ is nothing but $\mathcal{X}_\mathbf{u}$ augmented by the joint $\Pi_\mathbf{n}$.

Henceforth we focus on SMGs composed of four joints. Moreover, the four joints are either members of $\mathcal{S}_\mathbf{u}$ or of the $\mathsf{P}_{\mathbf{u}^\perp}$-type, where $\mathbf{u}^\perp$ is a unit vector normal to $\mathbf{u}$. Notice that the latter need not be identical to the unit vector $\mathbf{n}$ defining the Π joint of $\mathcal{S}_\mathbf{u}$. Furthermore, if any of the joints of $\mathsf{R}_\mathbf{u}$- or of $\mathsf{H}_\mathbf{u}$-type is repeated, then no two of the repeated joints are coaxial.

Lemma 8 *If* $\{\mathbf{u},\ \mathbf{v},\ \mathbf{w}\}$ *denotes an orthonormal triad, then using* $\mathsf{P}_\mathbf{v}$ *or* $\mathsf{P}_\mathbf{w}$ *to obtain the Schönflies motion subgroup* $\mathcal{X}(\mathbf{u})$ *is equivalent, i.e., the chains composed of* $\mathsf{P}_\mathbf{v}$ *joints are equivalent to the ones composed of* $\mathsf{P}_\mathbf{w}$ *joints.*

For example,

- $\mathsf{R}_\mathbf{u}\mathsf{R}_\mathbf{u}\mathsf{P}_\mathbf{v}\mathsf{P}_\mathbf{u}$ and $\mathsf{R}_\mathbf{u}\mathsf{R}_\mathbf{u}\mathsf{P}_\mathbf{w}\mathsf{P}_\mathbf{u}$ generate the same bond;
- $\mathsf{R}_\mathbf{u}\mathsf{R}_\mathbf{u}\mathsf{P}_\mathbf{u}\mathsf{P}_\mathbf{v}$ and $\mathsf{R}_\mathbf{u}\mathsf{R}_\mathbf{u}\mathsf{P}_\mathbf{u}\mathsf{P}_\mathbf{w}$ generate the same bond;
- $\mathsf{R}_\mathbf{u}\mathsf{P}_\mathbf{v}\mathsf{R}_\mathbf{u}\mathsf{P}_\mathbf{u}$ and $\mathsf{R}_\mathbf{u}\mathsf{P}_\mathbf{w}\mathsf{R}_\mathbf{u}\mathsf{P}_\mathbf{u}$ generate the same bond.

In the subsections below we list all independent kinematic chains producing $\mathcal{X}(\mathbf{u})$ with two, three and four joints of the set $\mathcal{S}_\mathbf{u}$.

4.1 Serial SMGs with R and P Pairs

A minimum list of SMGs producing $\mathcal{X}(\mathbf{u})$ and composed of only revolute and prismatic pairs obtained by using the foregoing rules is displayed in Table 1.

	Manipulator				Schematic Drawing
1	$\mathsf{R}_\mathbf{u}$	$\mathsf{R}_\mathbf{u}$	$\mathsf{R}_\mathbf{u}$	$\mathsf{P}_\mathbf{u}$	Fig. 3(b)
2	$\mathsf{R}_\mathbf{u}$	$\mathsf{R}_\mathbf{u}$	$\mathsf{P}_\mathbf{u}$	$\mathsf{P}_\mathbf{v}$	Fig. 3(i)
3	$\mathsf{R}_\mathbf{u}$	$\mathsf{P}_\mathbf{u}$	$\mathsf{P}_\mathbf{v}$	$\mathsf{P}_\mathbf{w}$	Fig. 3(n)

Table 1: Minimum list of $\mathcal{X}_\mathbf{u}$-generators with R and P pairs

4.2 Serial SMGs with R, P and H Pairs

As shown by Lee and Hervé [3], the Schönflies subgroup can be generated by means of sequences of kinematic pairs and a generic expression of the decomposition of the Schönflies subgroup into a product of four one-dimensional subgroups, which are associated with the single-dof lower kinematic pairs, e.g.,

$$\mathcal{X}(\mathbf{u}) = \mathcal{H}(\mathcal{A}_1, p_1) \bullet \mathcal{H}(\mathcal{A}_2, p_2) \bullet \mathcal{H}(\mathcal{A}_3, p_3) \bullet \mathcal{H}(\mathcal{A}_4, p_4) \tag{6}$$

with $\mathcal{A}_i$ passing through a point A_i of position vector $\mathbf{a}_i$ and parallel to the unit vector $\mathbf{u}$, p_i being the pitch of the ith helical pair. In the foregoing expression, every $\mathcal{H}$ subgroup comprises both the $\mathcal{R}$ and $\mathcal{P}$ subgroups, the former when the pitch vanishes, the latter when the pitch becomes unbounded.

In order to obtain the minimum list of serial SMGs composed of any combination of R, P and H pairs, we have to follow the rules introduced in Subsection 4.1 along with the ones stated below:

Lemma 9 *The four pitches in Eq. (6) must be distinct. Indeed, if $p_1 = p_2 = p_3 = p_4 = p$, then*

$$\mathcal{H}(\mathcal{A}_1, p_1) \bullet \mathcal{H}(\mathcal{A}_2, p_2) \bullet \mathcal{H}(\mathcal{A}_3, p_3) \bullet \mathcal{H}(\mathcal{A}_4, p_4) \in \mathcal{Y}(\mathbf{u}, p)$$

which is the 10th subgroup listed in Section 2. Each element of this subgroup is thus characterized by the two independent translations $t_\mathbf{v}$, $t_\mathbf{w}$ of directions perpendicular to $\mathbf{u}$, and either the rotation ϕ about this axis or the translation $t_\mathbf{u}$ in the direction of the axis.

Lemma 10 *If a Schönflies-motion-generating bond is composed of two H and two P pairs, and the former have identical pitches, with axes parallel to $\mathbf{u}$, then none of the directions of the latter must be perpendicular to $\mathbf{u}$.*

For a proof of this Lemma, the reader is referred to [3].

N°	Manipulator				Schematic		N°	Manipulator				Schematic
1	$R_\mathbf{u}$	$R_\mathbf{u}$	$R_\mathbf{u}$	$P_\mathbf{u}$	Fig. 3(b)		2	$R_\mathbf{u}$	$R_\mathbf{u}$	$R_\mathbf{u}$	$H_\mathbf{u}$	Fig. 3(a)
3	$R_\mathbf{u}$	$R_\mathbf{u}$	$P_\mathbf{u}$	$P_\mathbf{v}$	Fig. 3(i)		4	$R_\mathbf{u}$	$R_\mathbf{u}$	$P_\mathbf{u}$	$H_\mathbf{u}$	Fig. 3(d)
5	$R_\mathbf{u}$	$R_\mathbf{u}$	$P_\mathbf{v}$	$H_\mathbf{u}$	Fig. 3(j)		6	$R_\mathbf{u}$	$R_\mathbf{u}$	$H_\mathbf{u}$	$H_\mathbf{u}$	Fig. 3(c)
7	$R_\mathbf{u}$	$P_\mathbf{u}$	$P_\mathbf{v}$	$P_\mathbf{w}$	Fig. 3(n)		8	$R_\mathbf{u}$	$P_\mathbf{u}$	$P_\mathbf{v}$	$H_\mathbf{u}$	Fig. 3(m)
9	$R_\mathbf{u}$	$P_\mathbf{u}$	$H_\mathbf{u}$	$H_\mathbf{u}$	Fig. 3(f)		10	$R_\mathbf{u}$	$P_\mathbf{v}$	$P_\mathbf{w}$	$H_\mathbf{u}$	Fig. 3(o)
11	$R_\mathbf{u}$	$P_\mathbf{v}$	$H_\mathbf{u}$	$H_\mathbf{u}$	Fig. 3(l)		12	$R_\mathbf{u}$	$H_\mathbf{u}$	$H_\mathbf{u}$	$H_\mathbf{u}$	Fig. 3(e)
13	$P_\mathbf{u}$	$P_\mathbf{v}$	$P_\mathbf{w}$	$H_\mathbf{u}$	Fig. 4(e)		14	$P_\mathbf{u}$	$P_\mathbf{v}$	$H_\mathbf{u}$	$H_\mathbf{u}$	Fig. 4(a)
15	$P_\mathbf{u}$	$H_\mathbf{u}$	$H_\mathbf{u}$	$H_\mathbf{u}$	Fig. 3(h)		16	$P_\mathbf{v}$	$P_\mathbf{w}$	$H_\mathbf{u}$	$H_\mathbf{u}$	Fig. 3(p)
17	$P_\mathbf{v}$	$H_\mathbf{u}$	$H_\mathbf{u}$	$H_\mathbf{u}$	Fig. 3(k)		18	$H_\mathbf{u}$	$H_\mathbf{u}$	$H_\mathbf{u}$	$H_\mathbf{u}$	Fig. 3(g)

Table 2: Minimum list of $\mathcal{X}_\mathbf{u}$-generators with R, P, and H pairs

Table 2 shows a minimum list of $\mathcal{X}_\mathbf{u}$-generators with revolute, prismatic and screw pairs.

4.3 Serial SMGs with R, P, H and Π Joints

To come up with a minimum list of SMGs with R, P, H and Π joints, generating $\mathcal{X}(\mathbf{u})$, we have to follow the rules introduced in Subsections 4.1 and 4.2 plus the one below:

Lemma 11 *The SMG cannot contain more than two $\Pi_\mathbf{u}$, $\Pi_\mathbf{v}$ or $\Pi_\mathbf{w}$ pairs.*

Table 3 shows a minimum list of serial SMGs, in order of ascending complexity, composed of any combination of R, P, H and Π joints.

N°	Manipulator				K_N	K_L	K_J	K_B	K	Schematic
1	R_u	R_u	R_u	H_u	0.5076	0	0.5941	0	0.2754	Fig. 3(a)
2	R_u	R_u	R_u	P_u	0.5076	0	0.6425	0	0.2875	Fig. 3(b)
3	R_u	R_u	H_u	H_u	0.5076	0	0.6649	0	0.2931	Fig. 3(c)
4	R_u	R_u	P_u	H_u	0.5076	0	0.7133	0	0.3052	Fig. 3(d)
5	R_u	H_u	H_u	H_u	0.5076	0	0.7357	0	0.3108	Fig. 3(e)
6	R_u	P_u	H_u	H_u	0.5076	0	0.7841	0	0.3229	Fig. 3(f)
7	H_u	H_u	H_u	H_u	0.5076	0	0.8064	0	0.3285	Fig. 3(g)
8	P_u	H_u	H_u	H_u	0.5076	0	0.8548	0	0.3406	Fig. 3(h)
9	R_u	R_u	P_u	P_v	0.5076	0	0.7617	0.2091	0.3696	Fig. 3(i)
10	R_u	R_u	P_v	H_u	0.5076	0	0.7133	0.3109	0.3830	Fig. 3(j)
11	P_v	H_u	H_u	H_u	0.5076	0	0.8548	0.2091	0.3929	Fig. 3(k)
12	R_u	P_v	H_u	H_u	0.5076	0	0.7841	0.3109	0.4006	Fig. 3(l)
13	R_u	P_u	P_v	H_u	0.5076	0	0.8325	0.3109	0.4127	Fig. 3(m)
14	R_u	P_u	P_v	P_w	0.5076	0	0.8809	0.2668	0.4138	Fig. 3(n)
15	R_u	P_v	P_w	H_u	0.5076	0	0.8325	0.3291	0.4173	Fig. 3(o)
16	P_v	P_w	H_u	H_u	0.5076	0	0.9032	0.2668	0.4194	Fig. 3(p)
17	P_u	P_v	H_u	H_u	0.5076	0	0.9032	0.3109	0.4304	Fig. 4(a)
18	R_u	R_u	H_u	Π_u	0.7106	0.5358	0.4891	0	0.4339	Fig. 4(b)
19	R_u	R_u	P_u	Π_u	0.7106	0.5358	0.5167	0	0.4408	Fig. 4(c)
20	R_u	H_u	H_u	Π_u	0.7106	0.5358	0.5295	0	0.4440	Fig. 4(d)
21	P_u	P_v	P_w	H_u	0.5076	0	0.9516	0.3291	0.4471	Fig. 4(e)
22	R_u	P_u	H_u	Π_u	0.7106	0.5358	0.5571	0	0.4509	Fig. 4(f)
23	H_u	H_u	H_u	Π_u	0.7106	0.5358	0.5699	0	0.4541	Fig. 4(g)
24	P_u	H_u	H_u	Π_u	0.7106	0.5358	0.5976	0	0.4610	Fig. 4(h)
25	R_u	R_u	R_u	Π_v	0.7106	0.5358	0.4486	0.2091	0.4760	Fig. 4(i)
26	R_u	R_u	H_u	Π_v	0.7106	0.5358	0.4891	0.2091	0.4861	Fig. 4(j)
27	R_u	R_u	P_v	Π_v	0.7106	0.5358	0.5167	0.1893	0.4881	Fig. 4(k)
28	R_u	R_u	P_u	Π_v	0.7106	0.5358	0.5167	0.2091	0.4931	Fig. 4(l)
29	R_u	H_u	H_u	Π_v	0.7106	0.5358	0.5295	0.2091	0.4962	Fig. 4(m)
30	R_u	P_u	H_u	Π_v	0.7106	0.5358	0.5571	0.2091	0.5032	Fig. 4(n)
31	R_u	P_u	P_v	Π_v	0.7106	0.5358	0.5848	0.1893	0.5051	Fig. 4(o)
32	H_u	H_u	H_u	Π_v	0.7106	0.5358	0.5699	0.2091	0.5064	Fig. 4(p)
33	P_u	H_u	H_u	Π_v	0.7106	0.5358	0.5976	0.2091	0.5133	Fig. 5(a)

Next page

34	$\mathsf{P_v}$	$\mathsf{H_u}$	$\mathsf{H_u}$	$\Pi_{\mathbf{u}}$	0.7106	0.5358	0.5976	0.2091	0.5133	Fig. 5(b)
35	$\mathsf{R_u}$	$\mathsf{H_u}$	$\Pi_{\mathbf{u}}$	$\Pi_{\mathbf{u}}$	0.8299	0.7846	0.4470	0	0.5154	Fig. 5(c)
36	$\mathsf{R_u}$	$\mathsf{P_u}$	$\Pi_{\mathbf{u}}$	$\Pi_{\mathbf{u}}$	0.8299	0.7846	0.4664	0	0.5202	Fig. 5(d)
37	$\mathsf{H_u}$	$\mathsf{H_u}$	$\Pi_{\mathbf{u}}$	$\Pi_{\mathbf{u}}$	0.8299	0.7846	0.4753	0	0.5224	Fig. 5(e)
38	$\mathsf{P_u}$	$\mathsf{H_u}$	$\Pi_{\mathbf{u}}$	$\Pi_{\mathbf{u}}$	0.8299	0.7846	0.4947	0	0.5273	Fig. 5(f)
39	$\mathsf{R_u}$	$\mathsf{P_v}$	$\mathsf{H_u}$	$\Pi_{\mathbf{u}}$	0.7106	0.5358	0.5571	0.3109	0.5286	Fig. 5(g)
40	$\mathsf{P_v}$	$\mathsf{H_u}$	$\mathsf{H_u}$	$\Pi_{\mathbf{v}}$	0.7106	0.5358	0.5976	0.2871	0.5328	Fig. 5(h)
41	$\mathsf{P_v}$	$\mathsf{P_w}$	$\mathsf{H_u}$	$\Pi_{\mathbf{u}}$	0.7106	0.5358	0.6252	0.2668	0.5346	Fig. 5(i)
42	$\mathsf{R_u}$	$\mathsf{P_u}$	$\mathsf{P_v}$	$\Pi_{\mathbf{u}}$	0.7106	0.5358	0.5848	0.3109	0.5355	Fig. 5(j)
43	$\mathsf{R_u}$	$\mathsf{P_v}$	$\mathsf{P_w}$	$\Pi_{\mathbf{v}}$	0.7106	0.5358	0.5848	0.3109	0.5355	Fig. 5(k)
44	$\mathsf{R_u}$	$\mathsf{P_v}$	$\mathsf{H_u}$	$\Pi_{\mathbf{v}}$	0.7106	0.5358	0.5571	0.3494	0.5382	Fig. 5(l)
45	$\mathsf{P_u}$	$\mathsf{P_v}$	$\mathsf{H_u}$	$\Pi_{\mathbf{u}}$	0.7106	0.5358	0.6252	0.3109	0.5456	Fig. 5(m)
46	$\mathsf{P_v}$	$\mathsf{P_w}$	$\mathsf{H_u}$	$\Pi_{\mathbf{v}}$	0.7106	0.5358	0.6252	0.3109	0.5456	Fig. 5(n)
47	$\mathsf{P_u}$	$\mathsf{P_v}$	$\mathsf{H_u}$	$\Pi_{\mathbf{v}}$	0.7106	0.5358	0.6252	0.3494	0.5553	Fig. 5(o)
48	$\mathsf{R_u}$	$\mathsf{R_u}$	$\Pi_{\mathbf{v}}$	$\Pi_{\mathbf{v}}$	0.8299	0.7846	0.4187	0.1893	0.5556	Fig. 5(p)
49	$\mathsf{R_u}$	$\mathsf{R_u}$	$\Pi_{\mathbf{u}}$	$\Pi_{\mathbf{v}}$	0.8299	0.7846	0.4187	0.2091	0.5606	Fig. 6(a)
50	$\mathsf{R_u}$	$\mathsf{H_u}$	$\Pi_{\mathbf{v}}$	$\Pi_{\mathbf{v}}$	0.8299	0.7846	0.4470	0.1893	0.5627	Fig. 6(b)
51	$\mathsf{R_u}$	$\mathsf{P_v}$	$\Pi_{\mathbf{v}}$	$\Pi_{\mathbf{v}}$	0.8299	0.7846	0.4664	0.1732	0.5635	Fig. 6(c)
52	$\mathsf{R_u}$	$\mathsf{P_u}$	$\Pi_{\mathbf{v}}$	$\Pi_{\mathbf{v}}$	0.8299	0.7846	0.4664	0.1893	0.5675	Fig. 6(d)
53	$\mathsf{R_u}$	$\mathsf{H_u}$	$\Pi_{\mathbf{u}}$	$\Pi_{\mathbf{v}}$	0.8299	0.7846	0.4470	0.2091	0.5676	Fig. 6(e)
54	$\mathsf{H_u}$	$\mathsf{H_u}$	$\Pi_{\mathbf{v}}$	$\Pi_{\mathbf{v}}$	0.8299	0.7846	0.4753	0.1893	0.5698	Fig. 6(f)
55	$\mathsf{R_u}$	$\mathsf{P_u}$	$\Pi_{\mathbf{u}}$	$\Pi_{\mathbf{v}}$	0.8299	0.7846	0.4664	0.2091	0.5725	Fig. 6(g)
56	$\mathsf{P_u}$	$\mathsf{H_u}$	$\Pi_{\mathbf{v}}$	$\Pi_{\mathbf{v}}$	0.8299	0.7846	0.4947	0.1893	0.5746	Fig. 6(h)
57	$\mathsf{H_u}$	$\mathsf{H_u}$	$\Pi_{\mathbf{u}}$	$\Pi_{\mathbf{v}}$	0.8299	0.7846	0.4753	0.2091	0.5747	Fig. 6(i)
58	$\mathsf{R_u}$	$\mathsf{R_u}$	$\Pi_{\mathbf{v}}$	$\Pi_{\mathbf{w}}$	0.8299	0.7846	0.4187	0.2668	0.5750	Fig. 6(j)
59	$\mathsf{P_u}$	$\mathsf{H_u}$	$\Pi_{\mathbf{u}}$	$\Pi_{\mathbf{v}}$	0.8299	0.7846	0.4947	0.2091	0.5795	Fig. 6(k)
60	$\mathsf{P_v}$	$\mathsf{H_u}$	$\Pi_{\mathbf{u}}$	$\Pi_{\mathbf{u}}$	0.8299	0.7846	0.4947	0.2091	0.5795	Fig. 6(l)
61	$\mathsf{R_u}$	$\mathsf{H_u}$	$\Pi_{\mathbf{v}}$	$\Pi_{\mathbf{w}}$	0.8299	0.7846	0.4470	0.2668	0.5821	Fig. 6(m)
62	$\mathsf{R_u}$	$\mathsf{P_v}$	$\Pi_{\mathbf{v}}$	$\Pi_{\mathbf{w}}$	0.8299	0.7846	0.4664	0.2493	0.5825	Fig. 6(n)
63	$\mathsf{R_u}$	$\mathsf{P_u}$	$\Pi_{\mathbf{v}}$	$\Pi_{\mathbf{w}}$	0.8299	0.7846	0.4664	0.2668	0.5869	Fig. 6(o)
64	$\mathsf{H_u}$	$\mathsf{H_u}$	$\Pi_{\mathbf{v}}$	$\Pi_{\mathbf{w}}$	0.8299	0.7846	0.4753	0.2668	0.5891	Fig. 6(p)
65	$\mathsf{P_u}$	$\mathsf{H_u}$	$\Pi_{\mathbf{v}}$	$\Pi_{\mathbf{w}}$	0.8299	0.7846	0.4947	0.2668	0.5940	Fig. 7(a)
66	$\mathsf{P_v}$	$\mathsf{H_u}$	$\Pi_{\mathbf{v}}$	$\Pi_{\mathbf{v}}$	0.8299	0.7846	0.4947	0.2668	0.5940	Fig. 7(b)
67	$\mathsf{R_u}$	$\Pi_{\mathbf{u}}$	$\Pi_{\mathbf{v}}$	$\Pi_{\mathbf{v}}$	0.9000	0.9000	0.4026	0.1893	0.5980	Fig. 7(c)
Next page										

68	$\mathsf{P}_{\mathbf{v}}$	$\mathsf{H}_{\mathbf{u}}$	$\Pi_{\mathbf{u}}$	$\Pi_{\mathbf{v}}$	0.8299	0.7846	0.4947	0.2871	0.5990	Fig. 7(d)
69	$\mathsf{R}_{\mathbf{u}}$	$\Pi_{\mathbf{u}}$	$\Pi_{\mathbf{u}}$	$\Pi_{\mathbf{v}}$	0.9000	0.9000	0.4026	0.2091	0.6029	Fig. 7(e)
70	$\mathsf{H}_{\mathbf{u}}$	$\Pi_{\mathbf{u}}$	$\Pi_{\mathbf{v}}$	$\Pi_{\mathbf{v}}$	0.9000	0.9000	0.4244	0.1893	0.6034	Fig. 7(f)
71	$\mathsf{P}_{\mathbf{v}}$	$\mathsf{H}_{\mathbf{u}}$	$\Pi_{\mathbf{v}}$	$\Pi_{\mathbf{w}}$	0.8299	0.7846	0.4947	0.3109	0.6050	Fig. 7(g)
72	$\mathsf{R}_{\mathbf{u}}$	$\mathsf{P}_{\mathbf{v}}$	$\Pi_{\mathbf{u}}$	$\Pi_{\mathbf{v}}$	0.8299	0.7846	0.4664	0.3494	0.6076	Fig. 7(h)
73	$\mathsf{H}_{\mathbf{u}}$	$\Pi_{\mathbf{u}}$	$\Pi_{\mathbf{u}}$	$\Pi_{\mathbf{v}}$	0.9000	0.9000	0.4244	0.2091	0.6084	Fig. 7(i)
74	$\mathsf{R}_{\mathbf{u}}$	$\Pi_{\mathbf{v}}$	$\Pi_{\mathbf{w}}$	$\Pi_{\mathbf{w}}$	0.9000	0.9000	0.4026	0.2341	0.6092	Fig. 7(j)
75	$\mathsf{R}_{\mathbf{u}}$	$\Pi_{\mathbf{v}}$	$\Pi_{\mathbf{v}}$	$\Pi_{\mathbf{w}}$	0.9000	0.9000	0.4026	0.2493	0.6130	Fig. 7(k)
76	$\mathsf{H}_{\mathbf{u}}$	$\Pi_{\mathbf{v}}$	$\Pi_{\mathbf{w}}$	$\Pi_{\mathbf{w}}$	0.9000	0.9000	0.4244	0.2341	0.6146	Fig. 7(l)
77	$\mathsf{R}_{\mathbf{u}}$	$\Pi_{\mathbf{u}}$	$\Pi_{\mathbf{v}}$	$\Pi_{\mathbf{w}}$	0.9000	0.9000	0.4026	0.2668	0.6173	Fig. 7(m)
78	$\mathsf{H}_{\mathbf{u}}$	$\Pi_{\mathbf{v}}$	$\Pi_{\mathbf{v}}$	$\Pi_{\mathbf{w}}$	0.9000	0.9000	0.4244	0.2493	0.6184	Fig. 7(n)
79	$\mathsf{H}_{\mathbf{u}}$	$\Pi_{\mathbf{u}}$	$\Pi_{\mathbf{v}}$	$\Pi_{\mathbf{w}}$	0.9000	0.9000	0.4244	0.2668	0.6228	Fig. 7(o)

Table 3: Minimum list of $\mathcal{X}_{\mathbf{u}}$-generators with R, P, H, and Π joints, in order of ascending complexity

5 Complexity Evaluation

The 79 chains recorded in Table 3 are listed in order of ascending complexity, which is evaluated by means of a formulation provided in [14]. The complexity $K \in [0,1]$ of a kinematic chain is defined as a *convex combination* [16] of its various partial complexities, namely,

$$K = w_N K_N + w_L K_L + w_J K_J + w_B K_B \tag{7}$$

where $K_N \in [0,1]$ is the joint-number complexity, $K_L \in [0,1]$ the loop-complexity, $K_J \in [0,1]$ the joint-type complexity, and $K_B \in [0,1]$ the link diversity. A novel formulation of the latter is given in [18]. Furthermore, w_J, w_N, w_L, and w_B denote their corresponding weights, such that $w_J + w_N + w_L + w_B \; = \; 1$.

5.1 Joint-Number Complexity K_N

The joint-number complexity K_N is defined as:

$$K_N = 1 - \exp(-q_N N) \tag{8}$$

where N is the number of joints used in the chain at hand and q_N is the *resolution parameter*, to be adjusted according to the resolution required.

The joint-number complexity of the 79 chains is recorded in the third column of Table 3. As a Π-joint is composed of four revolute joints and the maximum number of Π-joints in the 79 chains under study is equal to three, the maximum number of joints N_{max} per chain is equal to 13, i.e., $N_{max} = 13$.

5.2 Loop Complexity K_L

The loop complexity K_L of a robot is defined as:

$$K_L = 1 - \exp(-q_L L); \quad L = l - l_m \tag{9}$$

where l is the number of kinematic loops in the robot, l_m is the minimum number of loops required to produce a special displacement group or subgroup and q_L is the corresponding resolution parameter. Within the scope of this paper $l_m = 0$, as the Schönflies displacement subgroup can be produced by a single-open-chain. Moreover, the maximum number of loops in the 79 chains under study is equal to three, i.e., $L_{max} = 3$. The loop complexity of the 79 chains is recorded in the fourth column of Table 3.

5.3 Joint-Type Complexity K_J

Joint-type complexity K_J is that associated with the type of LKPs used in a kinematic chain. As the 79 chains are composed of revolute, prismatic, helical and Π-joints only, the Π-joints being composed of four revolute joints, we define this complexity as

$$K_J = \frac{1}{n}\left[(n_R + 4n_\Pi)K_{G|R} + n_P K_{G|P} + n_H K_{G|H}\right] \tag{10}$$

where n_R, n_P, n_H and n_Π are the numbers of revolute, prismatic, helical and Π-joints, respectively, while $n = n_R + n_P + n_H + 4n_\Pi$ and $K_{G|\mathrm{x}}$ the geometric complexity of the pair x, as introduced in [18]: $K_{G|R} = 0.5234$, $K_{G|P} = 1$ and $K_{G|H} = 0.8064$. The joint-type complexity of the 79 chains is recorded in the fifth column of Table 3.

5.4 Link Diversity K_B

At the conceptual design stage, partial information about the geometric relations between neighboring joints is available. The five possible link layouts of the two joint axes of a binary link described in Fig. 2 were reported in [18]. As the joint axes of the 79 chains are either

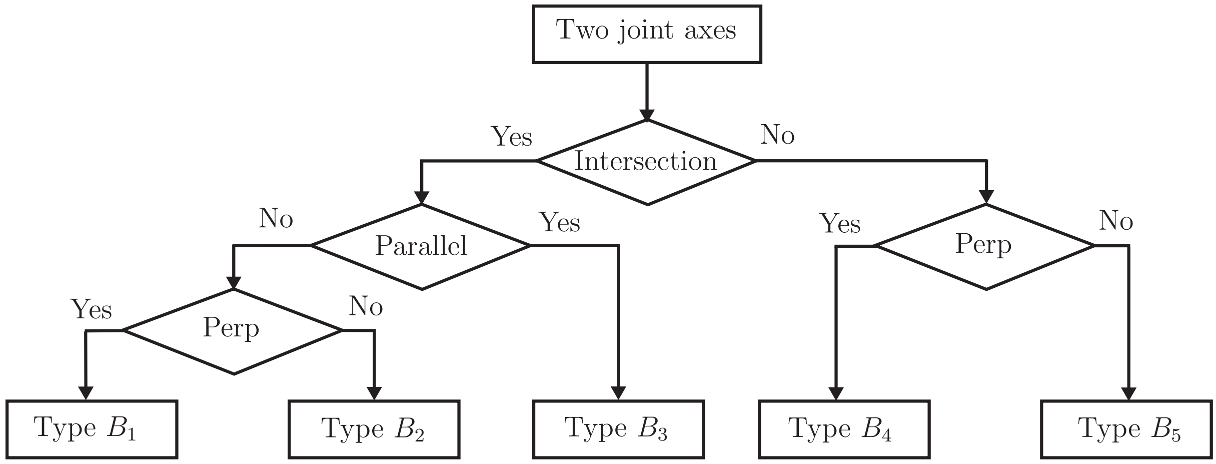

Figure 2: Binary tree displaying possible link topologies

parallel or orthogonal, we will distinguish only two types of link layouts in this paper, i.e., parallelism and perpendicularity. Besides, as Π-joints are composed of four revolute joints with parallel axes, it turns out that three constraints of parallelism have to be satisfied for their realization. Moreover, we borrow the concept of entropy from molecular thermodynamics and from information theory [19] to evaluate the effect of geometric-constraint diversity, at the conceptual stage. In this vein, we define the geometric-constraint diversity as:

$$K_B = \frac{B}{B_{max}} , \quad B = -\sum_{i=1}^{c} b_i \log_2(b_i) , \quad b_i = \frac{M_i}{\sum_{i=1}^{c} M_i} \tag{11}$$

where B is the entropy of the link layouts and B_{max} is the maximum possible value of B, with $B_{max} = \log_2(5) = 2.32$ bits [18], c is the number of distinct joint-constraint types used in a concept and M_i is the number of instances of each type of joint-constraints. The link diversity of the 79 chains is recorded in the sixth column of Table 3.

5.5 Definition of the Resolution Parameters

Two resolution parameters q_N and q_L were introduced above. These parameters provide an appropriate resolution for the complexity at hand. Since the foregoing formulation is intended to compare the complexities of 79 kinematic chains, it is reasonable to assign a complexity of 0.9 to the chain with maximum complexity, and hence, evaluate the normalizing constant, i.e., for $J = N$, L,

$$q_J = \begin{cases} -\ln(0.1)/J_{\max} & J_{\max} > 0; \\ 0 & J_{\max} = 0. \end{cases}$$

Consequently, $q_N = 0.1771$ and $q_L = 0.7675$.

Finally, the total complexity K of the 79 chains is recorded in the seventh column of Table 3

6 Conclusions

The paper reported on the conceptual design of the architecture of serial Schönflies-Motion Generators. A set of synthesis rules was proposed to determine a minimum list of chains capable of producing Schönflies motions. A minimum list of 79 *serial* Schönflies-Motion Generators composed of any possible combination of *revolute* R, *prismatic* P, *helical* H and Π joints was produced. Finally, a quantitative concept-evaluation framework, proposed in an earlier work, was applied to order the topologies obtained.

It is noteworthy that the $\mathcal{X}_{\mathbf{u}}$ chains bearing Π joints turn out to have the largest complexity, which corroborates the absence of this kind of joints in commercial SCARA systems of the serial type: with the exception of the ABB IRB660-1 robot, intended for moderately heavy loads, no other commercial SCARA system with Π joint is available in the market. One research robot of the SCARA type with a serial architecture was recently reported [20], which bears Π joints, as it is intended for the manipulation of heavy loads. We have included $\mathcal{X}_{\mathbf{u}}$ chains with Π joints because, even if for serial SMGs they do not offer a great advantage, this type of chains occur frequently in parallel SMGs. The advantage that these chains offer lies in their stiffness and their ability to produce pure translations between the two links to which they are attached.

7 Acknowledgements

This work was conducted with the support of the Idea to Innovation (I2I) Program of Canada's Natural Sciences and Engineering Research Council (NSERC). The authors acknowledge Vikram Chopra and Marie-Pier Landry-Dubé, undergraduate interns at McGill University's Centre for Intelligent Machines, for the production of the CAD models of the 79 kinematic chains. The partial support of the NSERC Design Engineering Chair at McGill University and of the James McGill Professorship of Mechanical Engineering, of which the fourth author is the holder, are dutifully acknowledged.

References

[1] Bottema, O. and Roth, B. (1979). *Theoretical Kinematics*, North Holland, Amsterdam.

[2] Hervé, J. (1999). "The Lie Group of Rigid Body Displacements, a Fundamental Tool for Mechanical Design," Mech. Mach. Theory, **34**, pp. 719–730.

[3] Lee, C-C. and Hervé, J.M. (2005). "On the Enumeration of Schoenflies Motion Generators," *The Ninth IFToMM International Symposium on Theory of Machines and Mechanisms*, Bucharest, Romania, September 1–4, SYROM 2005.

[4] Angeles, J. (2004). "The Qualitative Synthesis of Parallel Manipulators," ASME Journal of Mechanical Design, **126**(4), pp. 617–624.

[5] Angeles, J., Caro, S., Khan, W.A. and Morozov, A. (2006). "The Design and Prototyping of an Innovative Schönflies Motion Generator," *Proceedings of the IMechE Part C, Journal of Mechanical Engineering Science, special issue: Kinematics, Kinematic Geometry and their applications*, **220**(C7), July 2006, pp. 935–944.

[6] Lee, C-C. and Herve, J.M. (2006). "Translational Parallel Manipulators with Doubly Planar Limbs," Mech. Mach. Theory, **41**(4), pp. 433–455.

[7] Clavel, R. (1988). Delta, a Fast Robot with Parallel Geometry, *Proc. 18th Int. Symp. Industrial Robots*, Lausanne, pp. 91-100.

[8] Pierrot, F., Company, O. and Marquet, F. (2003). "H4: a High Speed 4 dof Parallel Robot." Synthesis, Modelling and Control Issues, IEEE Transactions on Robotics and Automation, **19**(3), June 2003, pp. 411–420.

[9] Dietmaier, P. (1992). "Inverse Kinematics of Manipulators with 3 Revolute and 3 Parallelogram Joints," *Proc. ASME 22nd Biennial Mechanisms Conference*, Scottsdale, AZ, Sept. 13–16, **45**, pp. 35-40.

[10] Hervé, J. M., and Sparacino, F. (1992). "Star, a New Concept in Robotics," *Proc. 3rd Int. Workshop on Advances in Robot Kinematics*, September 79, Ferrara, pp. 176-183.

[11] Wohlhart, K. (1992). "Displacement Analysis of the General Spatial Parallelogram Manipulator," *Proc. 3rd International Workshop on Advances in Robot Kinematics*, Ferrara, Italy, pp. 104-111.

[12] Macdonald, I.D. (1968). *The Theory of Groups*, Oxford University Press, London.

[13] Hervé, J. (1978). "Analyse structurelle des mécanismes par groupes de déplacements," Mech. Mach. Theory, **13**, pp. 437–450.

[14] Khan, W.A., Caro, S., Pasini, D. and Angeles, J. (2006a). "Complexity-Based Rules for the Conceptual Design of Robotic Architectures," 10^{th} *International Symposium on Advances in Robot Kinematics*, June 25–29, 2006, Ljubljana, Slovenia.

[15] Wohlhart, K., (1991). *Der homogene Paralleltrieb-Mechanismus*, Mathematica Pannonica, **2**(2), pp. 59–76.

[16] Boyd, S. and Vandenberghe, L. (2004). *Convex Optimization*, Cambridge University Press, Cambridge.

[17] Khan, W.A., Caro, S., Pasini, D. and Angeles, J. (2006b). "Complexity Analysis of Curves and Surfaces: Application to the Geometry Complexity of Lower Kinematic Pairs," Department of Mechanical Engineering and Centre for Intelligent Machines, Technical Report, McGill University, Montreal.

[18] Khan, W.A., Caro, S., Angeles, J. and Pasini, D. (2007). "A Formulation of Complexity Based Rules for the Preliminary Design Stage of Robotic Architectures," *the International Conference on Engineering Design*, August 28–31, Paris, France.

[19] Shannon, C.E. and Weaver, W. (1998). *The Mathematical Theory of Communication,* (first published in 1949), University of Illinois Press, Urbana and Chicago.

[20] Morozov, A. and Angeles, J. (2007). "The Mechanical Design of a Novel Schönflies-Motion Generator," *Robotics and Computer-Integrated Manufacturing*, **23**, pp. 82–93.

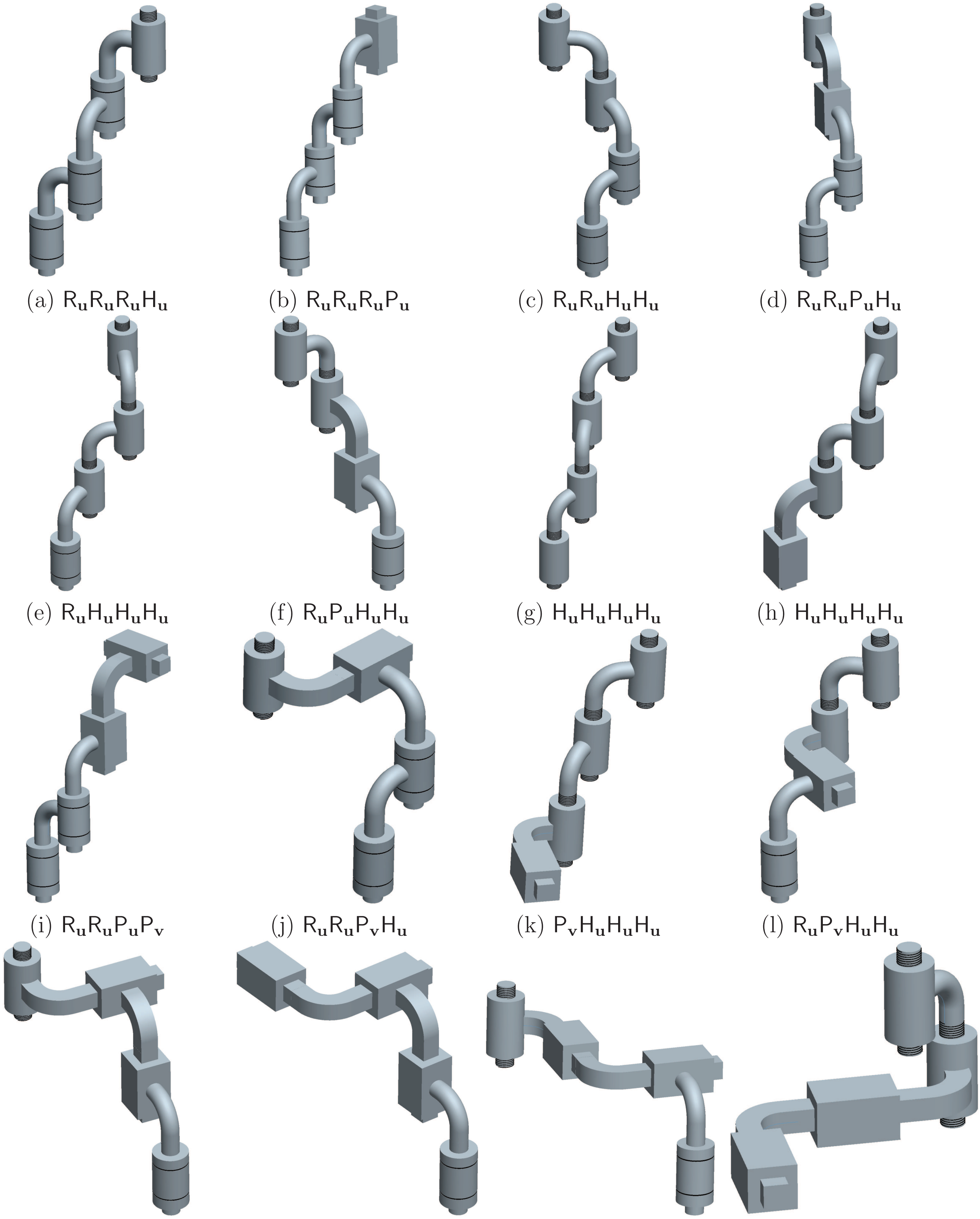

(a) $R_uR_uR_uH_u$ (b) $R_uR_uR_uP_u$ (c) $R_uR_uH_uH_u$ (d) $R_uR_uP_uH_u$

(e) $R_uH_uH_uH_u$ (f) $R_uP_uH_uH_u$ (g) $H_uH_uH_uH_u$ (h) $H_uH_uH_uH_u$

(i) $R_uR_uP_uP_v$ (j) $R_uR_uP_vH_u$ (k) $P_vH_uH_uH_u$ (l) $R_uP_vH_uH_u$

(m) $R_uP_uP_vH_u$ (n) $R_uP_uP_vP_w$ (o) $R_uP_vP_wH_u$ (p) $P_vP_wH_uH_u$

Figure 3: SCARA systems with R, P, H and Π pairs

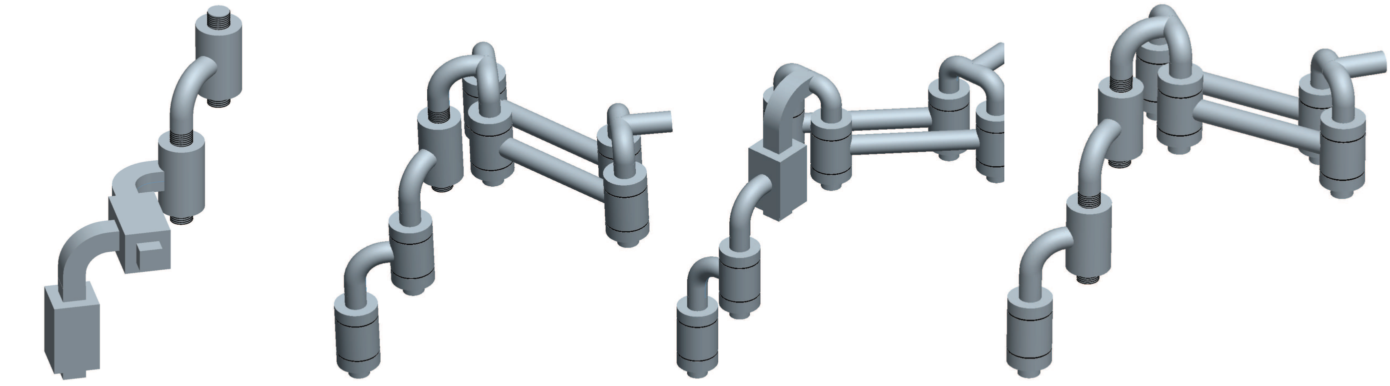

(a) $\mathsf{P_uP_vH_uH_u}$ (b) $\mathsf{R_uR_uH_u}\Pi_\mathbf{u}$ (c) $\mathsf{R_uR_uP_u}\Pi_\mathbf{u}$ (d) $\mathsf{R_uH_uH_u}\Pi_\mathbf{u}$

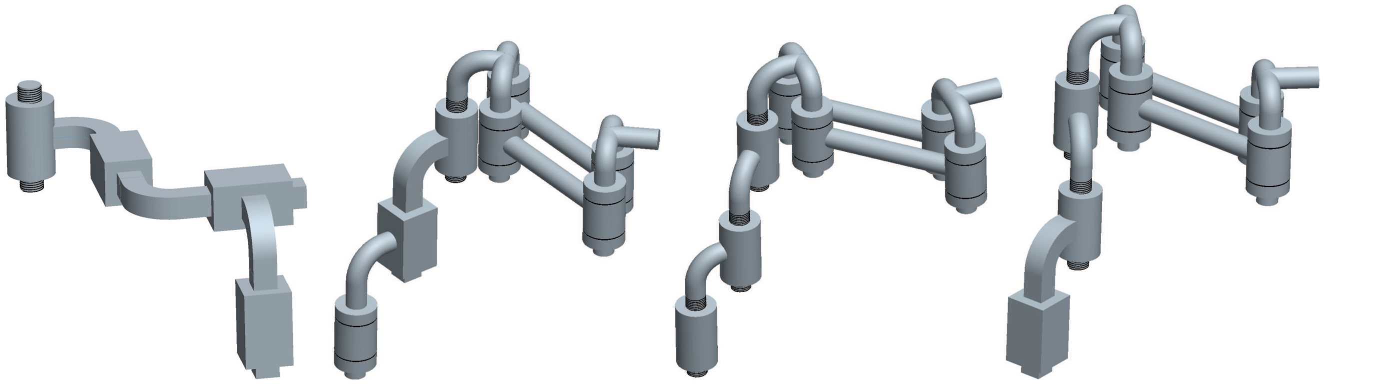

(e) $\mathsf{P_uP_vP_wH_u}$ (f) $\mathsf{R_uP_uH_u}\Pi_\mathbf{u}$ (g) $\mathsf{H_uH_uH_u}\Pi_\mathbf{u}$ (h) $\mathsf{P_uH_uH_u}\Pi_\mathbf{u}$

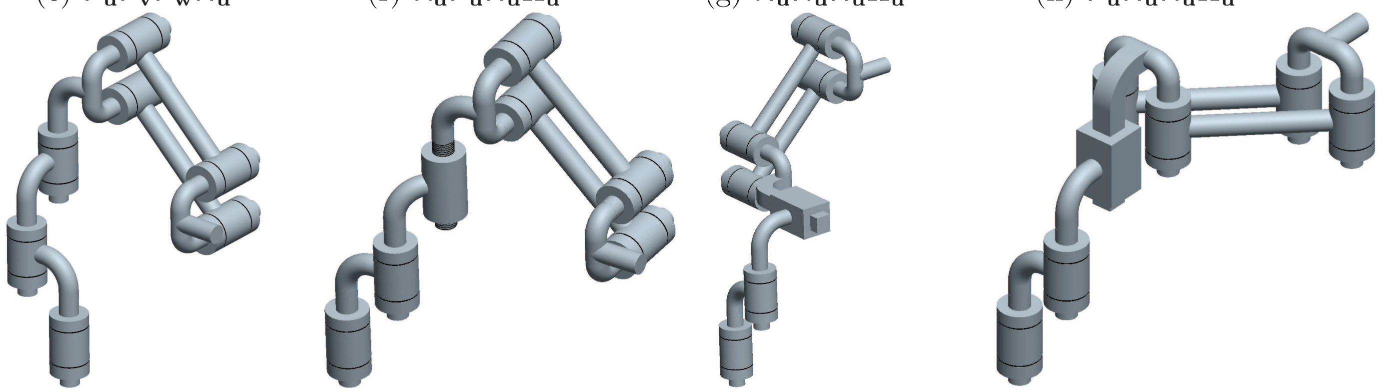

(i) $\mathsf{R_uR_uR_u}\Pi_\mathbf{v}$ (j) $\mathsf{R_uR_uH_u}\Pi_\mathbf{v}$ (k) $\mathsf{R_uR_uP_v}\Pi_\mathbf{v}$ (l) $\mathsf{R_uR_uP_u}\Pi_\mathbf{v}$

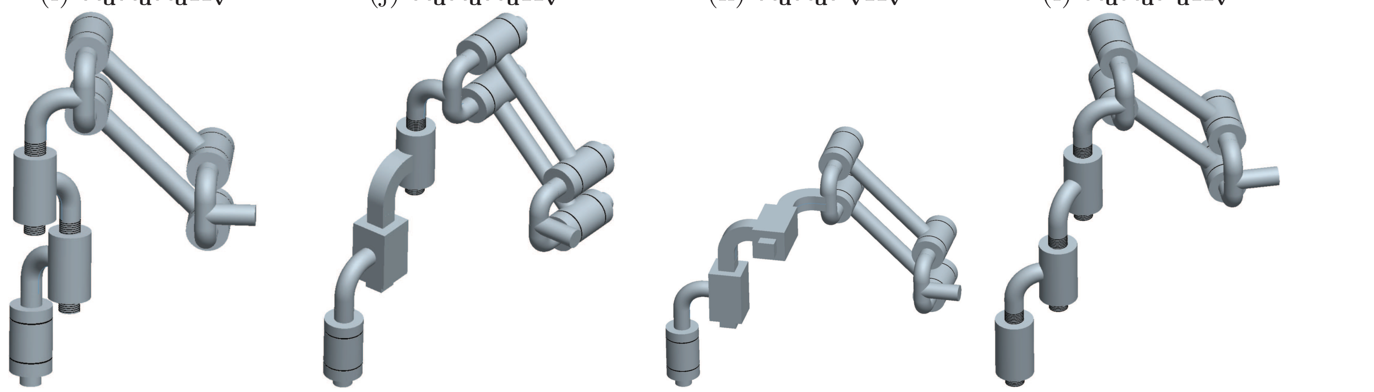

(m) $\mathsf{R_uH_uH_u}\Pi_\mathbf{v}$ (n) $\mathsf{R_uP_uH_u}\Pi_\mathbf{v}$ (o) $\mathsf{R_uP_uP_v}\Pi_\mathbf{v}$ (p) $\mathsf{H_uH_uH_u}\Pi_\mathbf{v}$

Figure 4: SCARA systems with R, P, H and Π pairs (Cont'd)

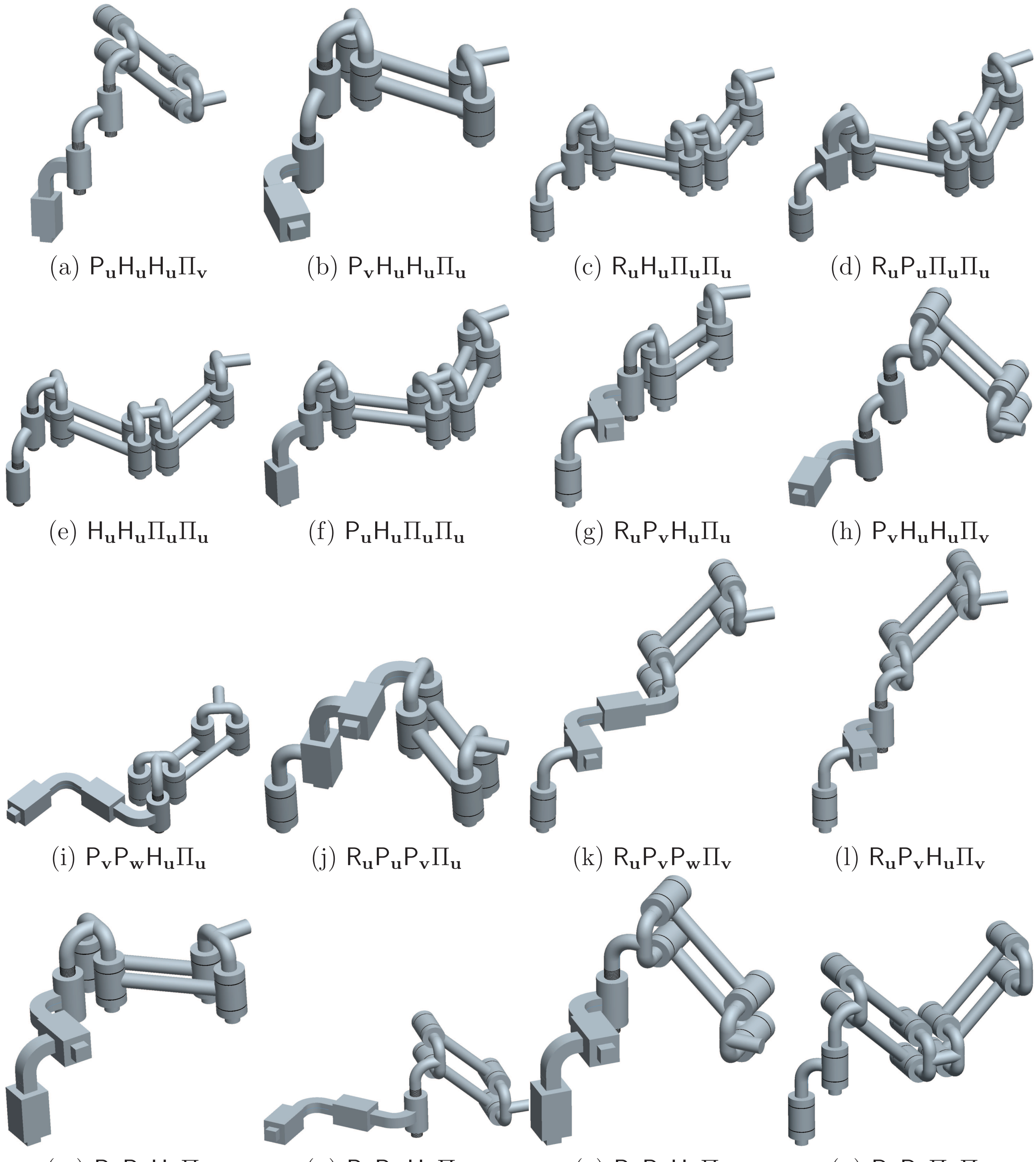

(a) $\mathsf{P_{\mathbf{u}}H_{\mathbf{u}}H_{\mathbf{u}}\Pi_{\mathbf{v}}}$ (b) $\mathsf{P_{\mathbf{v}}H_{\mathbf{u}}H_{\mathbf{u}}\Pi_{\mathbf{u}}}$ (c) $\mathsf{R_{\mathbf{u}}H_{\mathbf{u}}\Pi_{\mathbf{u}}\Pi_{\mathbf{u}}}$ (d) $\mathsf{R_{\mathbf{u}}P_{\mathbf{u}}\Pi_{\mathbf{u}}\Pi_{\mathbf{u}}}$

(e) $\mathsf{H_{\mathbf{u}}H_{\mathbf{u}}\Pi_{\mathbf{u}}\Pi_{\mathbf{u}}}$ (f) $\mathsf{P_{\mathbf{u}}H_{\mathbf{u}}\Pi_{\mathbf{u}}\Pi_{\mathbf{u}}}$ (g) $\mathsf{R_{\mathbf{u}}P_{\mathbf{v}}H_{\mathbf{u}}\Pi_{\mathbf{u}}}$ (h) $\mathsf{P_{\mathbf{v}}H_{\mathbf{u}}H_{\mathbf{u}}\Pi_{\mathbf{v}}}$

(i) $\mathsf{P_{\mathbf{v}}P_{\mathbf{w}}H_{\mathbf{u}}\Pi_{\mathbf{u}}}$ (j) $\mathsf{R_{\mathbf{u}}P_{\mathbf{u}}P_{\mathbf{v}}\Pi_{\mathbf{u}}}$ (k) $\mathsf{R_{\mathbf{u}}P_{\mathbf{v}}P_{\mathbf{w}}\Pi_{\mathbf{v}}}$ (l) $\mathsf{R_{\mathbf{u}}P_{\mathbf{v}}H_{\mathbf{u}}\Pi_{\mathbf{v}}}$

(m) $\mathsf{P_{\mathbf{u}}P_{\mathbf{v}}H_{\mathbf{u}}\Pi_{\mathbf{u}}}$ (n) $\mathsf{P_{\mathbf{v}}P_{\mathbf{w}}H_{\mathbf{u}}\Pi_{\mathbf{v}}}$ (o) $\mathsf{P_{\mathbf{u}}P_{\mathbf{v}}H_{\mathbf{u}}\Pi_{\mathbf{v}}}$ (p) $\mathsf{R_{\mathbf{u}}R_{\mathbf{u}}\Pi_{\mathbf{v}}\Pi_{\mathbf{v}}}$

Figure 5: SCARA systems with R, P, H and Π pairs (Cont'd)

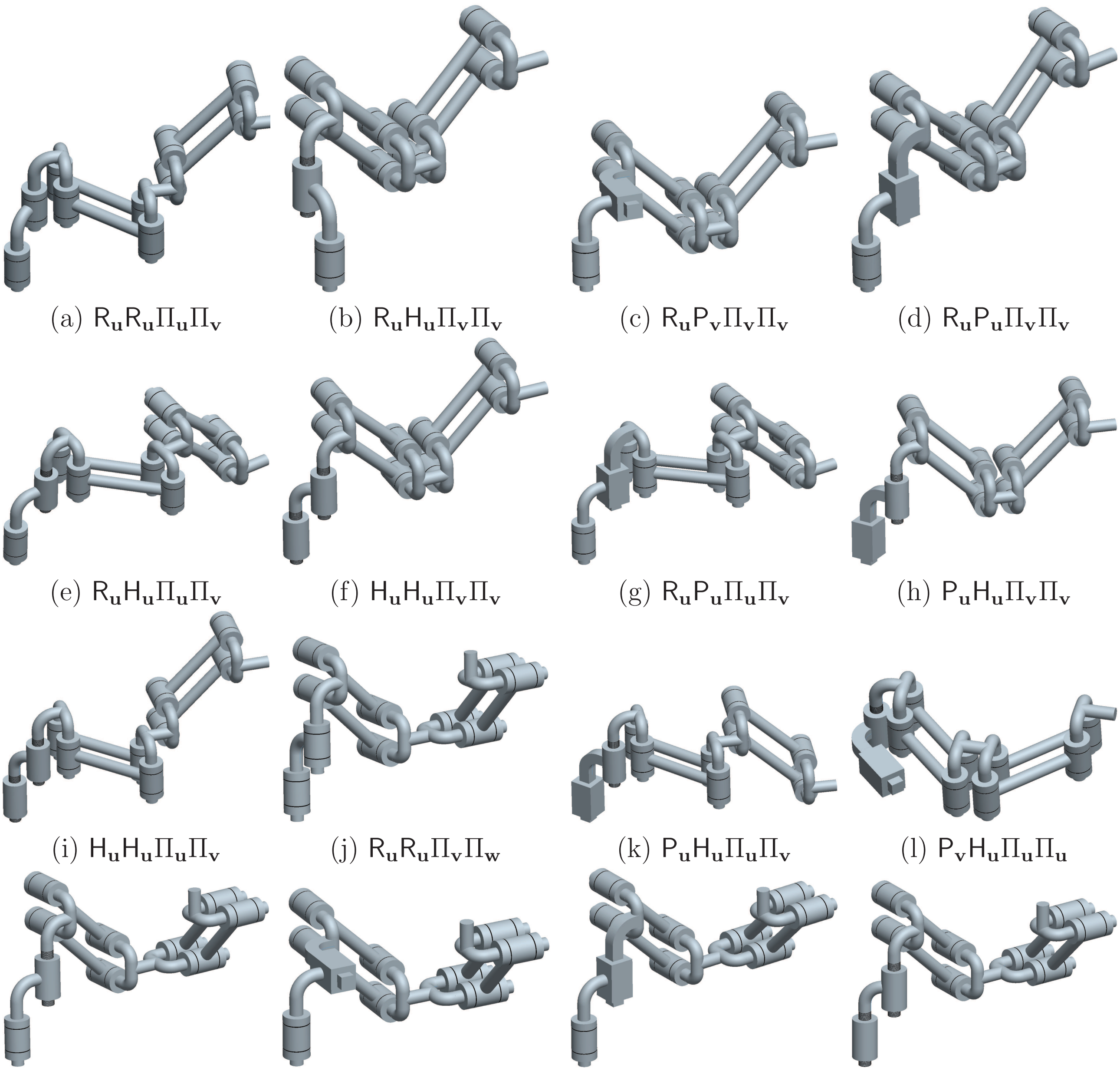

(a) $\mathsf{R}_\mathbf{u}\mathsf{R}_\mathbf{u}\Pi_\mathbf{u}\Pi_\mathbf{v}$ (b) $\mathsf{R}_\mathbf{u}\mathsf{H}_\mathbf{u}\Pi_\mathbf{v}\Pi_\mathbf{v}$ (c) $\mathsf{R}_\mathbf{u}\mathsf{P}_\mathbf{v}\Pi_\mathbf{v}\Pi_\mathbf{v}$ (d) $\mathsf{R}_\mathbf{u}\mathsf{P}_\mathbf{u}\Pi_\mathbf{v}\Pi_\mathbf{v}$

(e) $\mathsf{R}_\mathbf{u}\mathsf{H}_\mathbf{u}\Pi_\mathbf{u}\Pi_\mathbf{v}$ (f) $\mathsf{H}_\mathbf{u}\mathsf{H}_\mathbf{u}\Pi_\mathbf{v}\Pi_\mathbf{v}$ (g) $\mathsf{R}_\mathbf{u}\mathsf{P}_\mathbf{u}\Pi_\mathbf{u}\Pi_\mathbf{v}$ (h) $\mathsf{P}_\mathbf{u}\mathsf{H}_\mathbf{u}\Pi_\mathbf{v}\Pi_\mathbf{v}$

(i) $\mathsf{H}_\mathbf{u}\mathsf{H}_\mathbf{u}\Pi_\mathbf{u}\Pi_\mathbf{v}$ (j) $\mathsf{R}_\mathbf{u}\mathsf{R}_\mathbf{u}\Pi_\mathbf{v}\Pi_\mathbf{w}$ (k) $\mathsf{P}_\mathbf{u}\mathsf{H}_\mathbf{u}\Pi_\mathbf{u}\Pi_\mathbf{v}$ (l) $\mathsf{P}_\mathbf{v}\mathsf{H}_\mathbf{u}\Pi_\mathbf{u}\Pi_\mathbf{u}$

(m) $\mathsf{R}_\mathbf{u}\mathsf{H}_\mathbf{u}\Pi_\mathbf{v}\Pi_\mathbf{w}$ (n) $\mathsf{R}_\mathbf{u}\mathsf{P}_\mathbf{v}\Pi_\mathbf{v}\Pi_\mathbf{w}$ (o) $\mathsf{R}_\mathbf{u}\mathsf{P}_\mathbf{u}\Pi_\mathbf{v}\Pi_\mathbf{w}$ (p) $\mathsf{H}_\mathbf{u}\mathsf{H}_\mathbf{u}\Pi_\mathbf{v}\Pi_\mathbf{w}$

Figure 6: SCARA systems with R, P, H and Π pairs (Cont'd)

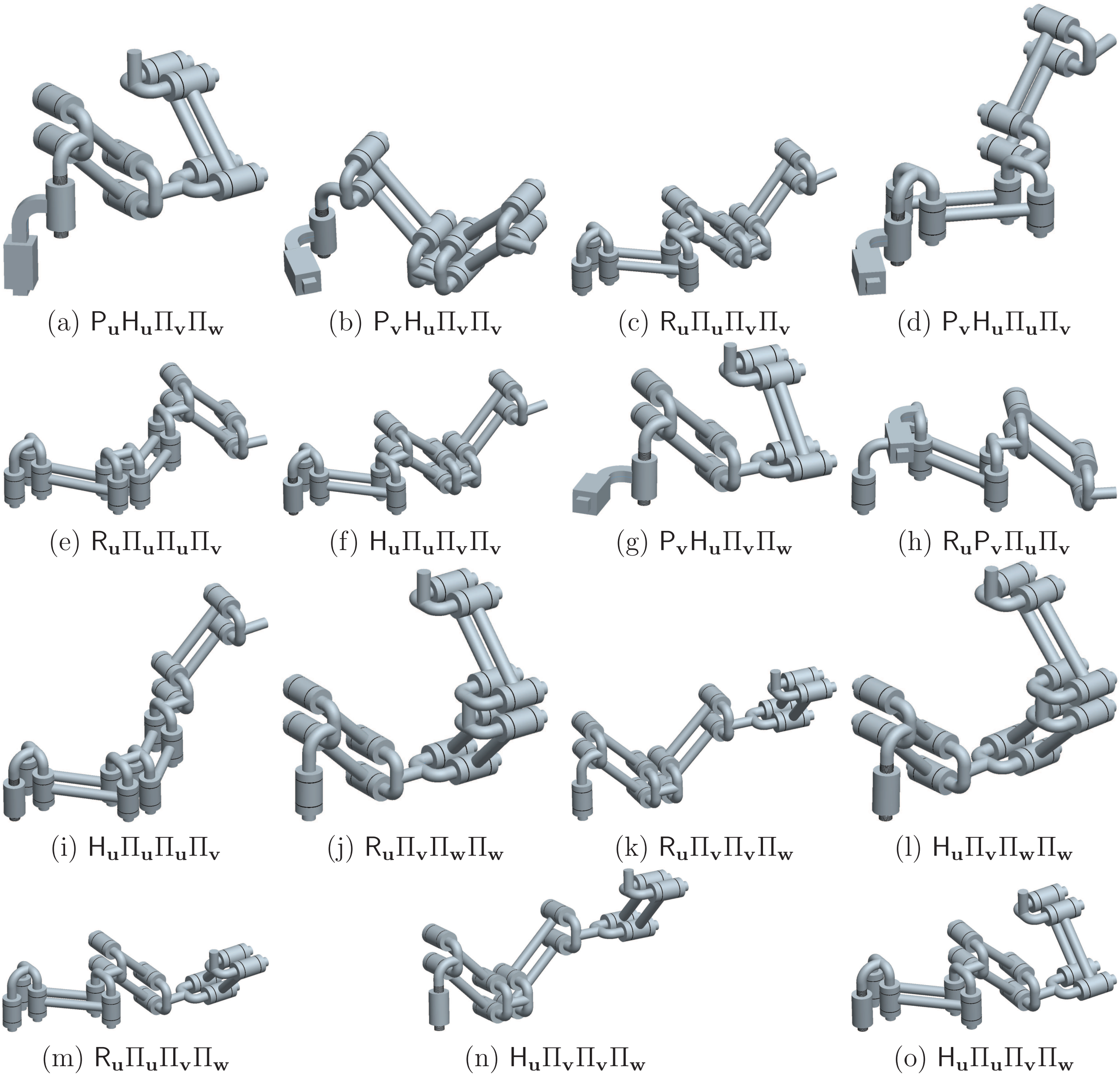

Figure 7: SCARA systems with R, P, H and Π pairs (Cont'd)